Aligned collagen–GAG matrix as a 3D substrate for Schwann cell migration and dendrimer-based gene delivery

ARTICLE *in* JOURNAL OF MATERIALS SCIENCE MATERIALS IN MEDICINE · MAY 2014

Impact Factor: 2.59 · DOI: 10.1007/s10856-014-5224-2 · Source: PubMed

5 AUTHORS, INCLUDING:

Simon James Archibald
Integra LifeSciences
28 PUBLICATIONS **1,157** CITATIONS
SEE PROFILE

Dzmitry Shcharbin
National Academy of Sciences of Belarus
103 PUBLICATIONS **1,115** CITATIONS
SEE PROFILE

Maria Bryszewska
University of Lodz
278 PUBLICATIONS **4,240** CITATIONS
SEE PROFILE

Journal of Materials Science Materials in Medicine. 2014. *Just Accepted*.

Final version is available from:
http://link.springer.com/article/10.1007/s10856-014-5224-2

DOI: 10.1007/s10856-014-5224-2

Authors are very thankful to *Springer*
and *Journal of Materials Science: Materials in Medicine*
for possibility to publish authors' *initial* version.

Aligned collagen-GAG matrix as a 3D substrate for Schwann cell migration and dendrimer-based gene delivery

Antos Shakhbazau [1,2]*, Simon J. Archibald [3], Dzmitry Shcharbin [4], Maria Bryszewska [5], Rajiv Midha [1,2]

[1] – *Department of Clinical Neuroscience, Faculty of Medicine, University of Calgary, Calgary, Canada;*
[2] – *Hotchkiss Brain Institute, University of Calgary, Calgary, Canada;*
[3] – *Integra LifeSciences Corporation, Plainsboro, NJ, USA.*
[4] – *Institute of Biophysics and Cell Engineering, National Academy of Sciences of Belarus, Minsk, Belarus;*
[5] – *Department of General Biophysics, University of Lodz, Lodz, Poland.*

*** Corresponding Author**. Department of Clinical Neuroscience, University of Calgary, HMRB 109-3330 Hospital Drive NW T2N4N1, Calgary, Canada.

Abstract
The development of artificial off-the-shelf conduits that facilitate effective nerve regeneration and recovery after repair of traumatic nerve injury gaps is of fundamental importance. Collagen-glycosaminoglycan (GAG) matrix mimicking Schwann cell basal lamina has been proposed as a suitable and biologically rational substrate for nerve regeneration. In the present study, we have focused on the permissiveness of this matrix type for Schwann cell migration and repopulation, as these events play an essential role in nerve remodeling. We have also demonstrated that Schwann cells cultured within collagen-GAG matrix are compatible with non-viral dendrimer-based gene delivery, that may allow conditioning of matrix-embedded cells for future gene therapy applications.

Keywords
collagen-GAG matrix, artificial nerve graft, Schwann cells, migration, dendrimers, transfection.

Introduction

Peripheral nerve injury is a serious health concern for society, affecting 2.8% of trauma patients, many of whom acquire life-long disability (Noble et al., 1998). The peripheral nervous

system is known to have some regenerative potential after injury, however, severe nerve injuries are associated with complete loss of tissue or lengthy scar within the nerve trunk that prevent regenerating axons from effectively innervating the distal nerve stump. The repair of most nerve injuries entails reconstruction of a nerve gap once the scar is resected. Nerve autografting, the gold standard of surgical care (Millesi et al., 1972), still has inherent flaws, such as donor site morbidity created in procuring the nerve graft leading to loss of function and occasionally neuroma pain (Belkas et al., 2005). Moreover, autologous nerve grafting has reached a plateau in the potential restoration of functional outcome, and further improvement may only be achieved through the application of technological innovation. For this reason, many investigators have been evaluating synthetic nerve conduits as an improved alternative. Tubes based on biodegradable materials, such as collagen, have enjoyed success in rat and primate models of nerve repair (Archibald et al., 1991; Archibald et al., 1995; Kemp et al., 2009). Integra LifeSciences has recently developed a propriety method for the synthesis of a collagen-glycosaminoglycan (GAG) matrix derived from collagen type 1, whose microscopic geometry (pore size and longitudinal array) closely mimics Schwann cell basal lamina (SCBL).

Schwann cells (SCs) are the specific myelinating cells in the PNS, that promote clearance of inhibitory debris after nerve injury during Wallerian degeneration. They also orchestrate axonal regeneration by the production and presentation of growth factors to the regenerating axonal growth cones. The success of an artificial nerve graft is inevitably dependent on effective migration and colonization by Schwann cells (SCs) (Hudson et al., 1972; Zhao et al., 1992), that provide neurotrophic factors (Brushart, 1991; Richardson, 1991), as well as favorable cell and endoneurial tube surface adhesion molecules (Martini, 1994) to regenerating axons (Fu et al., 1997). Indeed, Schwann cells lead regenerating axons via the regenerating nerve tissue bridge and failure of their migration is associated with abortive axonal regeneration (Chen et al., 2005). Genetic modification has also been considered as a method to enhance SCs' regenerative potential by increasing production of neurotrophic factors or inducing their migratory properties (Hu et al., 2005; Lavdas et al., 2006; Shakhbazau et al., 2012a). We herein hypothesize that the synthetic SCBL mimic in the form of a collagen-glycosaminoglycan (GAG) matrix is permissive for Schwann cell migration and also compatible with a virus-free genetic engineering approach.

Materials and methods

Schwann cell isolation and culture

Schwann cells (SCs) were isolated from sciatic nerves of P2 Lewis rats according to minor modifications of established protocols (Komiyama et al., 2003; Walsh *et al.*, 2009). Sciatic nerves were excised, stripped of their epineurium, and cut into 1 mm^2 pieces. Nerve segments were placed on poly-D-lysine coated 35 mm culture dishes in DMEM/F12 medium supplemented with 10% FBS, 1% penicillin/streptomycin and 0,25 µg/mL Fungizon for 3 days, allowing removal of fibroblasts from the nerve tissue by cell migration. Media was then changed to serum-free DMEM containing 1% N2, 10 ng/mL heregulin-1β, 4 µM forskolin (hereafter referred to as SC medium) for another 3 days to stimulate SC outgrowth. At day 6, the nerve fragments were removed from the dish and explanted onto another 35-mm dish in SC-medium with 2.5% FBS. The explant procedure was repeated until little outgrowth of fibroblasts was observed, then the explants were discarded and all dishes containing SCs were purified in serum-free SC-medium. Purity of SC cultures was assessed by p75 and GFAP immunolabeling and a heregulin exclusion test. Cells were routinely maintained on plastic tissue culture flasks and plates (Falcon) at 37˚C in a humidified atmosphere containing 5% CO_2/95% air.

Collagen-GAG matrix preparation

The collagen-GAG matrix was fabricated similarly to a previously published process (Yannas et al., 1989). To prepare the matrix, a collagen and chondroitin-6-sulfate proteoglycan suspension was dispensed into the collagen conduits. The filled conduits were frozen under controlled conditions and then lyophilized to produce a highly porous matrix with an axially oriented pore structure. The implants were sterilized with ethylene oxide and supplied ready for use. Collagen-GAG matrix tubes were cryosectioned (Leica Microsystems Inc., Richmond Hill, ON, Canada) into 60 µm-thick sections at -23 °C and mounted on Superfrost slides (Fisher Scientific), or sectioned with scalpel blade into ~0.5 mm-thick three-dimensional (3D) fragments.

SC co-culture with collagen-GAG matrix

Matrix sections and fragments were washed extensively with HBSS (6 times), then SC medium, then equilibrated in SC medium for 2-3 days. After pretreatment, sections and fragments were placed into wells of 96-well plate for SC co-culture. SCs were labeled with CellTracker CM-DiI (Invitrogen, Burlington, ON, Canada) according to the manufacturer's guidelines. Briefly, cells were trypsinized from culture vessels and resuspended in serum-free SC-medium, containing 1 μM DiI staining solution. Following incubation for 20 min in the dark, cells were washed three times in DMEM and seeded on matrix fragments in 96-well plate at concentrations of $1x10^5$, $2x10^5$, or $1x10^6$ per mL in standard SC medium with 15% serum, or on 60 μm cryosections in 90 mm Petri dish. To evaluate SC attachment and growth, matrix fragments and cryosections were observed by microscopy (Olympus BX51, Center Valley, PA, USA) for DiI fluorescence, or fixed in 2% paraformaldehyde (PFA) and submitted for p75 immunohistochemistry.

Transfection reagents

The vector used in transfection experiments was pLVHTM (Addgene plasmid 12247), generated by Didier Trono (Szulc et al., 2006) and obtained from Addgene (Cambridge, USA). pLVHTM plasmid was propagated in the provided *E. coli* strain Stbl3 and isolated by Plasmid Maxi kit (Qiagen) according to the manufacturer's instructions. Purified plasmids DNA with an A260/A280 ratio of 1.8 were used for transfection. PAMAM-NH_2 dendrimers of 4th generation (PAMAM G4, MW 14,214, diameter 4–4.5 nm) were purchased from Sigma-Aldrich, USA.

Biophysical characterization of dendriplexes

Plasmid/dendrimer complexation was assessed using ethidium bromide intercalation assay and particle size and zeta-potential measurements. Ethidium bromide (EB) was added to the vector solution (0.6 nmol/L) in the final concentration of 7 μmol/l and its fluorescence was read using a LS-55B spectrofluorimeter (Perkin-Elmer, USA). The excitation wavelength was 484 nm, and the excitation and emission slits were 10 nm. The emission spectra were recorded between 500 and 700 nm and the position of emission maximum was determined. The 'dye-vector' complex was then titrated with a dendrimer and changes in the fluorescence parameters (intensity and $\lambda^{em}_{\max}$) were recorded. The data graph was modified so that the changes in fluorescence intensity of the EB-plasmid complex when dendrimers were added were presented as

$$F^{rev} = \frac{F^{complex} - F^{pureEB}}{F_0^{complex} - F^{pureEB}} \qquad (1),$$

where $F^{complex}$ is the fluorescence of EB-plasmid in the presence of dendrimer, F^{pureEB} is the fluorescence of pure (free) EB, and $F_0^{complex}$ is the fluorescence of the EB-plasmid complex in the absence of dendrimer when EB is fully bound by the plasmid.

The particle size and zeta-potential of pLVHTM/dendrimer complex was measured using a Zetasizer Nano ZS (Malvern Instruments Ltd., UK) at 25 °C in a disposable Malvern plastic cuvette. Charge ratios for the dendriplexes studied was 5:1 (P:N).

Transfection procedures

SC transfections (n=3 for each condition) were performed as described earlier (Shakhbazau et al., 2012c). Dendrimers were diluted to a concentration of 20 mM in terms of nitrogen residues, complexes with pLVHTM plasmid DNA were prepared in 50 μL of 150 mM NaCl solution at a charge ratio of 1:1-1:1,2 and the mixtures were vortexed and incubated for 15 min at room temperature. Transfections of plastic-adherent or matrix-embedded SC were carried out in 96-well plates in SC culture medium by 5 h exposure to PAMAM-plasmid complexes (10% v/vol of total medium). GFP fluorescence was monitored by microscopy (Olympus BX51, Center Valley, PA, USA) 24 h after transfection.

Assessment of SC migration on the collagen-GAG matrix

To assess SC migration onto the matrix as a natural extension of their growth-permissive surface, SCs were seeded into the empty well and allowed to grow to a confluent monolayer (See Suppl. Fig. 1 for the outline). The empty matrix section was then placed on the monolayer and co-cultured for 1 week. Matrix section was then removed, rinsed and placed onto the glass slide for microscopic examination. To observe whether SC migrate from the matrix after co-culture as a confirmation of their motility and viability, matrix fragments and cryosections earlier seeded with SC were rinsed in SC medium and moved aseptically to the new empty wells of 96-well plate. Migrated cells were observed on the well surface microscopically and by DiI fluorescence. To assess *ex vivo* SC migration from fresh sciatic nerve explants into the matrix tube, sciatic nerve explants from Lewis male rats were cut into 2-3 mm segments, which were labeled with DiI and attached into the indents at the end of the collagen tube containing the SCBL matrix within. At 1, 2, 3 and 4 weeks time points, tubes were opened and migration of DiI+ cells was monitored by fluorescent microscopy. For *in vivo* assessment of SC migration into the matrix tube, tubes were implanted into sciatic nerve as described below, and SC migration was evaluated by p75 immunohistochemistry.

Animals

Lewis rats weighing 225–250 g (Charles River, QC, Canada) were used in animal experiments (as detailed below). Animals were maintained in a temperature and humidity controlled environment with a 12-h light/dark cycle. Food (Purina, Mississauga, ON, Canada) and water were available *ad libitum*. Surgical interventions were carried out under inhalation anaesthetic (Isofluroane, 99.9% Halocarbon Laboratories, River Edge, NJ, USA) and pain control was provided by means of i.p. or oral administration of buprenorphine (30 μg/kg). Surgical procedures were carried out aseptically, and standard microsurgical techniques were used with an operating microscope (Wild M651; Wild Leitz, Willowdale, ON, Canada). Animals were sacrificed at endpoint under deep anaesthesia using an overdose of intracardiac Euthanol (Bimeda–MTC, Cambridge, ON, Canada). All efforts were made to minimize suffering and animal numbers by using appropriate protocols. The protocol was approved and monitored by the University of Calgary animal care committee and adhered strictly to guidelines set by the Canadian Council on Animal Care.

Surgical procedures

All animals were operated bilaterally for both sciatic nerve excision or matrix implantation experiments. Sciatic nerve was exposed at mid-thigh level after splitting the biceps femoris muscle and either excised for *ex vivo* SC migration screening, or transected ~1 cm proximal to the trifurcation with a small segment removed to create a 5-mm gap. After one week denervation, in a second surgery all animals received a 7 mm implant of collagen-GAG matrix tube separately at each proximal (n=4) and distal (n=4) ends of sciatic nerve, secured with 9–0 proline microsutures (see Figure 4E). Wounds were closed in layers, and the animals were housed as described above with appropriate painkiller administration (4 days), until sacrifice at 2 weeks time point.

Immunohistochemistry

At 2 weeks following surgery and matrix implantation, collagen-GAG matrix tubes along with their attached sciatic nerves were excised and fixed overnight in 2% paraformaldehyde in phosphate-buffered saline (PBS). Samples were washed three times in PBS, cryoprotected in 30% sucrose and embedded in optimal cutting temperature (OCT) compound (Sakura Fine technical Co., Torrance, CA, USA). 24 μm longitudinal sections were cut with a cryostat (Leica Microsystems Inc., Richmond Hill, ON, Canada) at -23 °C and mounted on Superfrost slides (Fisher Scientific). Immunolabeling of cryosections or PFA-fixed matrix fragments was made as follows. Sections or fragments were blocked/permeabilized with 2% BSA/ 0,3% Triton-X100 in PBS and incubated overnight in primary anti-p75 antibody (Santa Cruz, USA). Following 3x wash with PBS, slides were incubated with secondary antibody (Alexa Fluor 488, Molecular Probes, USA) and Hoechst solution (1:2000) for 3 h. Slides were then washed and coverslipped using Fluorosave reagent (Calbiochem, San Diego, CA, USA) and viewed under a fluorescence microscope (Olympus BX51, Center Valley, PA, USA). Omission of primary or secondary antibody was used as negative control for the staining process.

Statistical analysis

Differences between groups were analyzed using a one-way ANOVA with statistical significance accepted at $P<0.05$. All results are presented as the mean ± SEM.

Results and discussion

Overcoming length limitations in peripheral nerve repair poses an ongoing challenge. Several biodegradable tubes are currently approved for human use, but notably the efficacy and thus the indications for the use of all the tubes marketed to date are limited to short gap nerve defects (Schlosshauer et al., 2007). Experimental studies reveal that endowing the tube lumen with a growth supportive matrix represents a promising strategy to enhance regenerative success. Schwann cell basal lamina is a particularly potent substrate for neurite promotion (Armstrong et al., 2008; Webber et al., 2010). Conduit filled with collagen-GAG matrix has recently been proposed as a superior regeneration-promoting material (Chamberlain et al., 1998; Chamberlain et al., 2000; Lee *et al.*, 2012), whose 3D microarchitecture promotes cell migration via junction interactions and nerve graft maturation after axonal regrowth (Chamberlain *et al.*, 1998; Harley et al., 2008). Permissivity of any nerve guidance conduit for Schwann cell migration is of particular importance as they replenish nerve tissue by proliferating and produce a favorable environment for axonal regrowth (Zochodne, 2008). Moreover, SC have been recently identified as a central organizer of the complex cellular post-injury response via Raf/MEK/ERK signaling pathway, which is indispensible for peripheral nerve repair (Harrisingh et al., 2004; Napoli et al., 2012). In the current study, we have therefore specifically focused on the properties of this type of matrix as a substrate for *in vit*ro and *in vivo* SC migration and non-viral engineering.

In our *in vitro* experiments, SC seeding and migration was assessed on cryosections and fragments of collagen-GAG matrix, with major focus on the latter as the 3D fragments retained transparency, allowed multiple washing, were compatible with 96-well plate format, and maximally preserved initial matrix structure. Both sections and fragments were populated with DiI-positive Schwann cells at 1 and 2 week time points (Fig. 1A,B). Schwann cells retained their morphology and sent processes across the matrix, suggesting that the presently formulated matrix permits attachment and growth of the cells. The 3D structure of the matrix was populated within multiple layers through the whole depth of the fragment, which was allowed for microscopic observation by the transparent nature of the matrix. The data suggest that the matrix permits seeding and/or penetration of SCs into the deep inner areas of structure. Despite the demonstrated robust survival, the expansion of purified SC in the 3D matrix was limited (Suppl. Fig. 2) and in the longer term co-cultures, the surface around the matrix was preferred for SC growth *in vitro* (Suppl. Fig. 3). Immunolabeling for p75-NTR (specific SC marker) at 4 weeks time point further confirms SC survival and ability to retain proper phenotype after prolonged incubation on SCBL matrix sections (Fig. 2).

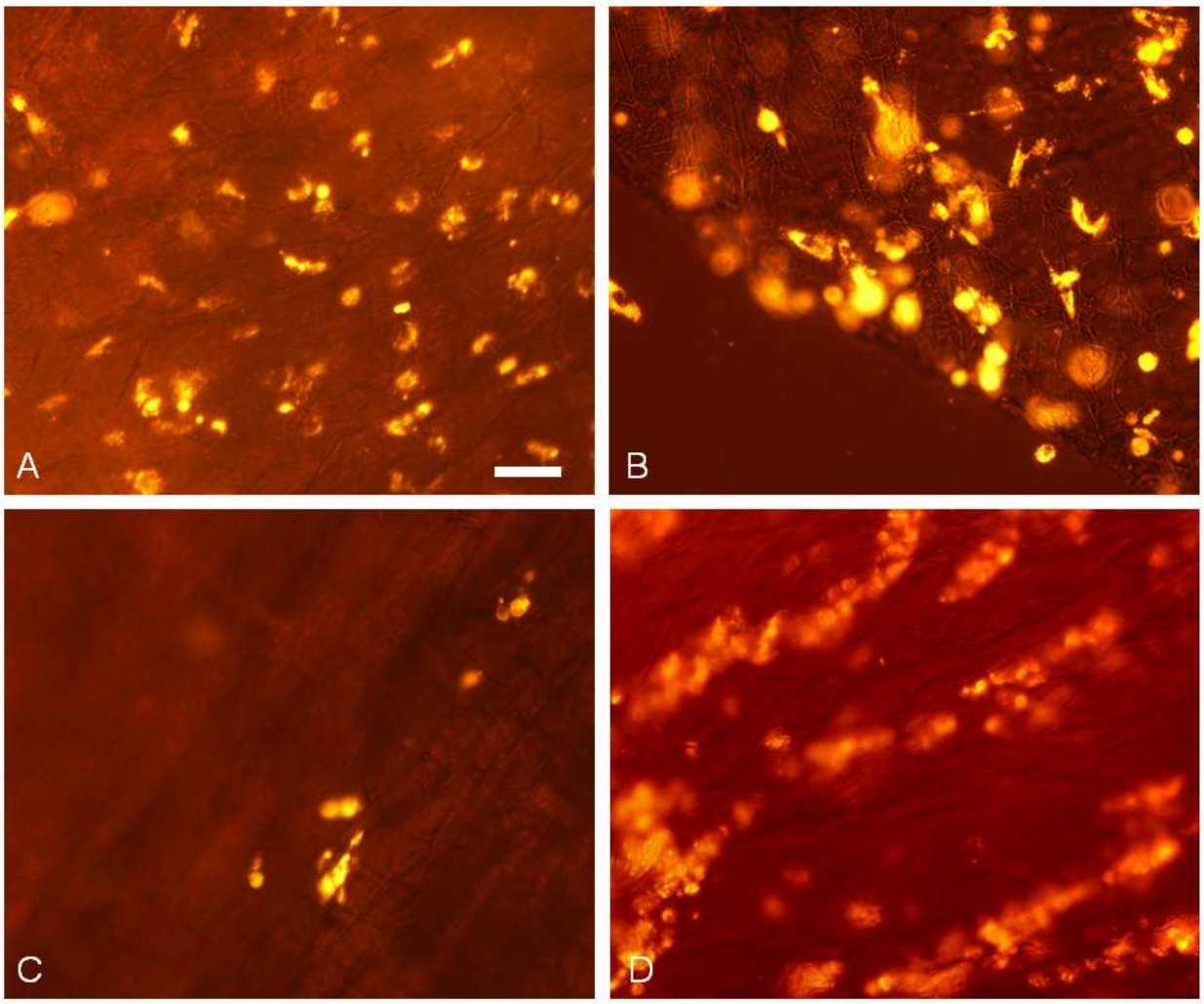

Figure 1. Purified cultured Schwann cells on collagen-GAG matrix *in vitro* (100x total magnification, all SC labeled with DiI, fluorescence and transmitted light). A, SCs seeded on 3D matrix fragment, scale bar 50 μm; B, SCs seeded on 60 um matrix cryosection; C, SCs migrated onto empty matrix fragment from plastic-adherent monolayer; D, SCs form linear bands along the axial structure of 3D matrix fragment.

The ability of SCs to migrate from the pre-seeded matrix to the surrounding surface is an additional evidence of their viability (example in Suppl. Fig. 2B). Importantly, DiI-positive SCs also showed natural ability to migrate onto the matrix sections and fragments from the plastic-adherent monolayer (Fig. 1C). Demonstrated attachment of SCs to the matrix (as opposed to seeding the cells on top of the matrix section) provides evidence of the SCBL matrix being naturally populated by SCs as a permissive growth substrate extension.

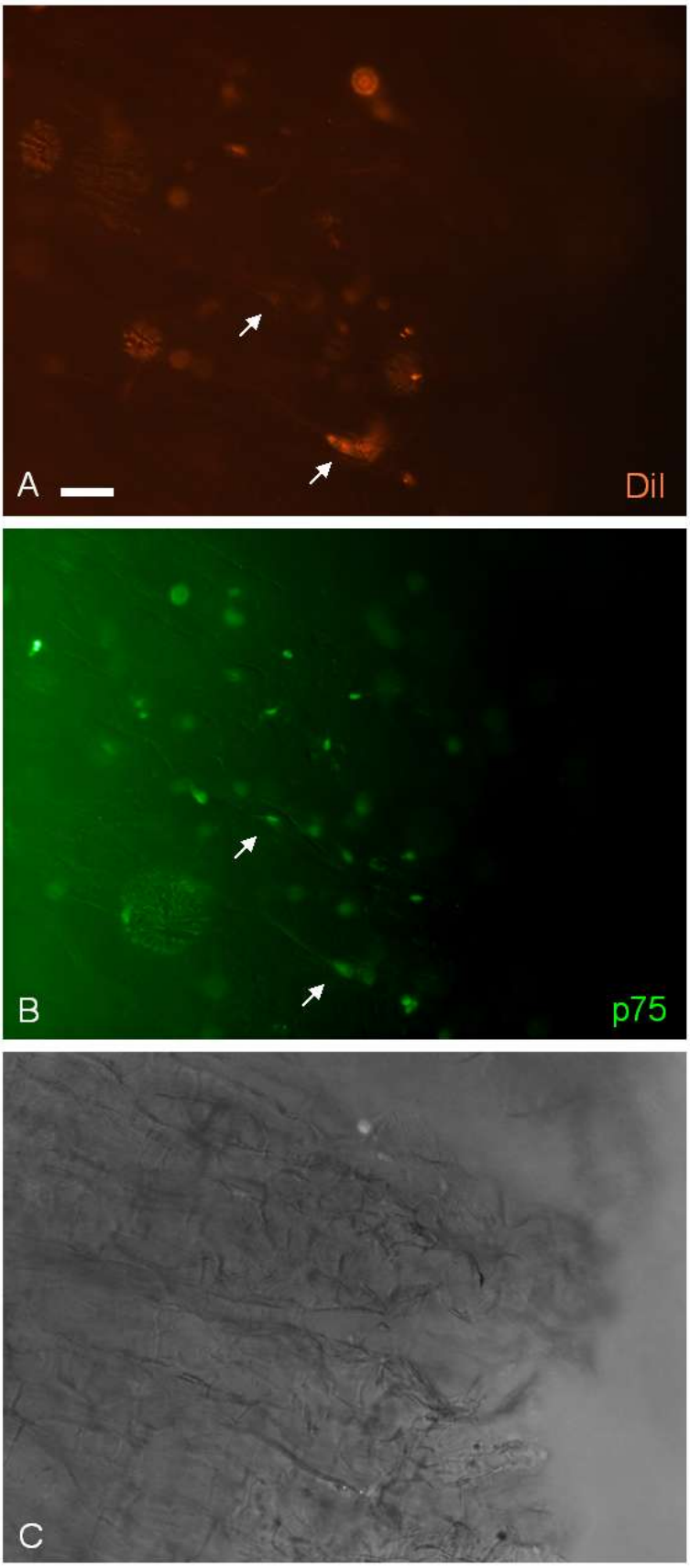

Figure 2. p75 immunolabeling of purified Schwann cells on collagen-GAG matrix *in vitro* at 4 weeks time point (100x total magnification, scale bar 50 µm, all SCs labeled with DiI). A, SCs retain DiI fluorescence; B, SCs are positive for specific marker p75 (arrows indicate representative SCs); C, 3D structure of the same matrix fragment (transmitted light).

SC migratory properties are influenced by the matrix composition and structure. The main constituent of our biomaterial of interest was collagen, a major structural protein which has been widely used in the biomedical research because of its low antigenicity, good mechanical properties and ability for biodegradation (Archibald et al., 1991). Supplementation of GAGs to collagen modulates matrix microenvironment by its involvement in adhesion, migration, proliferation, and differentiation of cells, which also influences growth factor and cytokine production in the regenerative area (Pieper et al., 2000). Chondroitin-6-sulfate proteoglycan is present in the natural SCBL and is over-expressed by Schwann cells after nerve injury, modulating Schwann cell migration in the affected site (Liu et al., 2006). The axial alignment of collagen-GAG matrix was shown to allow directed SC migration along the 3D linear paths and formation of long patterned columns to support axon outgrowth and myelination (Zhao *et al.*, 1992). We found that in some areas of the matrix SCs have grouped along the longitudinal structure of the matrix fibers in a manner that resembles bands of Bungner (Fig. 1D), which guide axons through the injury site back to their targets (Zochodne, 2008). This effect in the *in vitro* model of matrix seeding with purified cultured SC may suggest that alignment of SC into the linear columns is guided by axial microarchitecture of the matrix and occurs independently from signals of other cell types.

Our next *in vitro* experiments were focused on SC migration along the longitudinal structure of the matrix from the terminally attached DiI-labeled fragments of fresh sciatic nerve (details in Suppl. Fig. 4). Fig. 3A shows cell migration at 1, 2, 3, and 4 week time points, suggesting high migratory permissivity of the matrix. Main migration front in this experimental setup was moving at an approximate speed of 1 mm/week, while various scattered cells were observed ahead of the front in the matrix. A sub-population of the cells demonstrated SC morphology and were p75-positive (Fig. 3B, 3C), while most of the cells were putatively fibroblasts. The latter were recently shown to invade the injury zone first and independently of SC signals and create permissive conditions for the formation of a regeneration bridge (Napoli *et al.*, 2012; Parrinello et al., 2010). Fibroblasts then orchestrate SC migration into the injury site via ephrin-B/EphB2-mediated cell sorting, mediated by Sox2-dependent N-cadherin relocalization (Parrinello *et al.*, 2010).

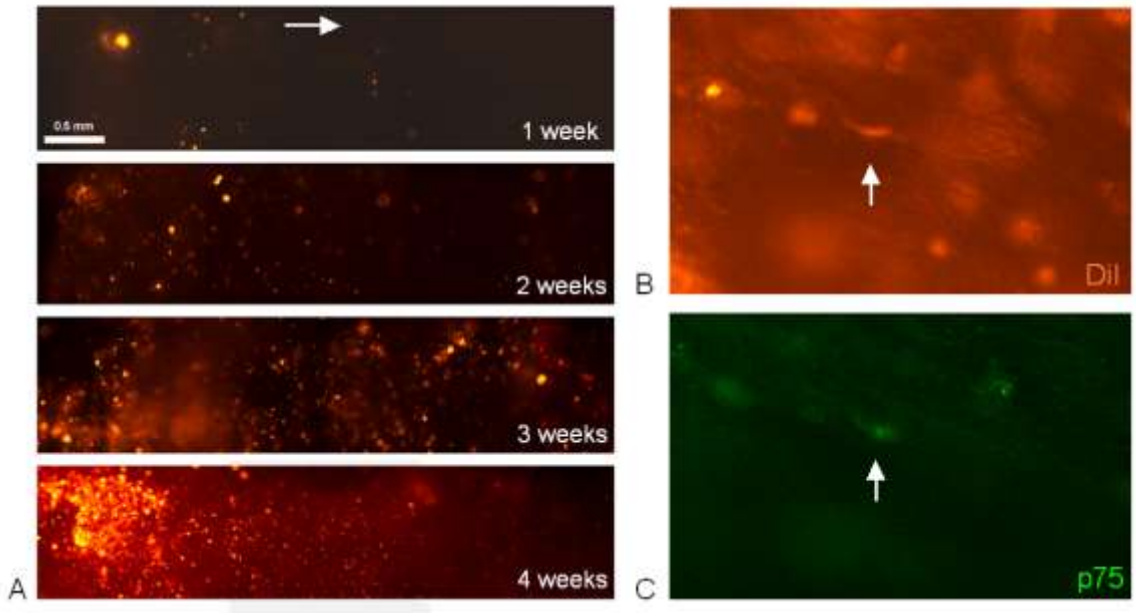

Figure 3. Cell migration from DiI-labeled fragments of fresh sciatic nerve into the collagen-GAG matrix tube *in vitro.* A, overall extent of migration (40x total magnification, arrow indicates direction of cell migration from the nerve fragment) . A fraction of migrated cells appear to be SCs (arrows in B and C, 100x), as evidenced by bipolar elongated morphology (B) and positivity for p75 (C).

To validate our model in the *in vivo* setting, we have analyzed SC migration into the matrix tubes separately from proximal and distal ends of transected sciatic nerve after 1 week of denervation (Fig. 4). After 2 weeks post-implantation, both proximal and distal collagen-GAG

implants were heavily infiltrated with mostly p75-negative cells, abundantly clustering in the central areas of the matrix (Fig 4C,D). This is in line with the concept of fibroblast and inflammatory cell invasion and conditioning of regenerative cable microenvironment for nerve remodeling with SCs participation. Areas populated with SCs were also observable along the whole length of the 7 mm implant tube, as evidenced by cell morphology and p75 immunopositivity (Fig. 4A,B). SCs appear to readily infiltrate and adhere to the matrix surface using the collagen-GAG fiber topology as a permissive substrate. Abundant migration from the nerve, as opposed to quite limited expansion of purified SCs seeded on the matrix *in vitro* (Suppl. Fig.2), may reflect the pre-conditioning of the matrix surface with fibroblast-derived growth-supportive molecules and factors *in vivo*. Note that migrating SCs *in vivo* acquire their characteristic morphology in the matrix microarchitecture much more easily compared to *in vitro* co-culture, which can also be explained by fibroblast-driven remodeling of the regenerative microenvironment (Parrinello *et al.*, 2010). Nerve injury is known to rapidly affect Schwann cells by activating ERK signaling pathway, which in turn leads to an increase in the expression of factors inducing SC proliferation (calcitonin/calcitonin-related polypeptide, TGFβ1, plasminogen activator) and migration (CD44, gap junction protein α1, cadherin 2, cofilin 1, integrin α3, etc) (Napoli *et al.*, 2012). Quantification of SC infiltration from proximal and distal ends of transected nerve revealed a trend for higher amounts of SCs invading from the distal part (Fig 4F), which is expected as SCs are known to proliferate actively in the denervated area of the nerve which is undergoing Wallerian degeneration (Harrisingh *et al.*, 2004; Napoli *et al.*, 2012; Zochodne, 2008).

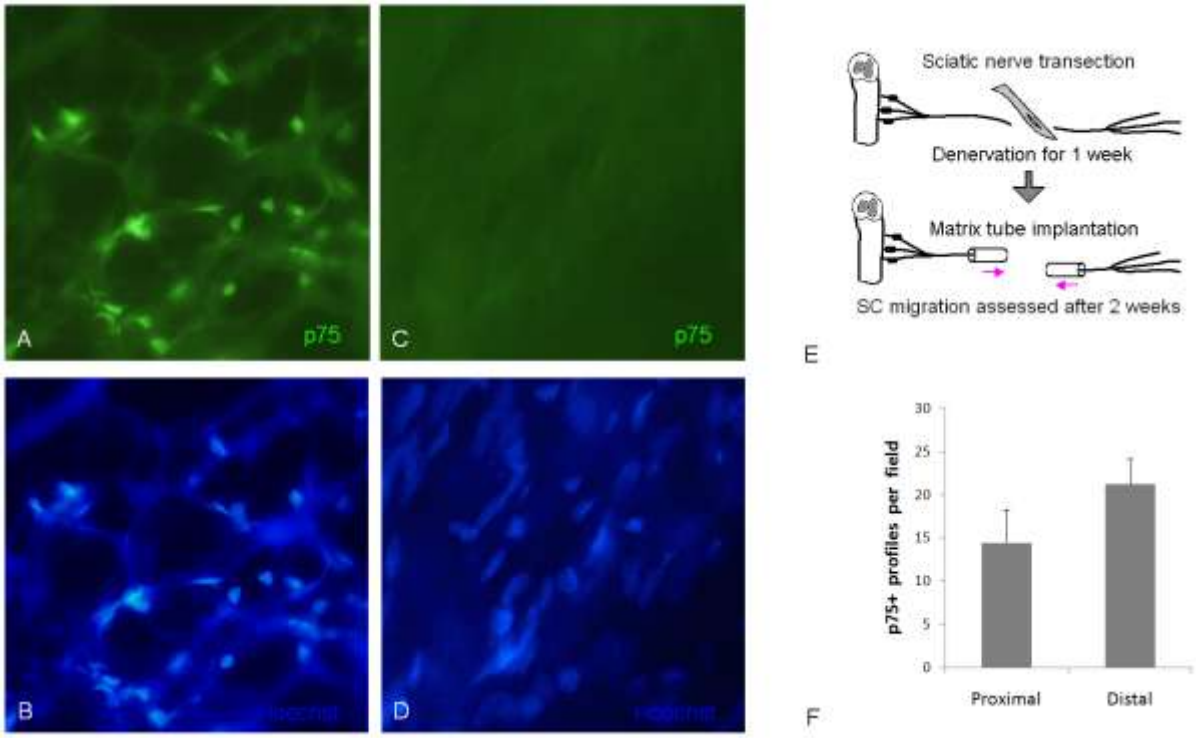

Figure 4. Cell migration into the collagen-GAG matrix tubes *in vivo.* A-B, representative image of SC infiltration area (note the preserved 3D matrix structure). C-D, representative image of an area occupied by p75-negative cells (nuclei stained by Hoechst). E, *in vivo* experiment outline. F, quantification of average numbers of SC per 400x magnification field.

Our next aim was to assess compatibility of SC culture in collagen-GAG matrix with the novel virus-free approach for gene delivery. SC engineering for PSA-NCAM over-expression has been earlier reported to increase their capacity for migration (Bachelin et al., 2010; Lavdas et al., 2006), and a number of factors were able to enhance their regenerative potential (Hu et al., 2005; Shakhbazau et al., 2012a; Weidner et al., 1999). The downside of the commonly used viral systems, rightly recognized as an effective gene carrier, is potential immunogenicity, risk of genome destabilization and oncogene activation after provirus integration, and the potential of wild type reversion. In search for non-viral vehicles, a number of compounds with unique

transfection properties have been synthesized and validated in different cell types (Hanafi et al., 2013; Luo et al., 2011; Mandke et al., 2012; Sharma et al., 2012; Yamada et al., 2013). Gene carriers used in our study were 4th generation (G4) PAMAM-NH_2 dendrimers, characterized by polyamidoamine molecules branching from the central core with a cationic multivalent surface created by amine termini. G4 PAMAM-NH_2 dendrimers possess 64 surface amino groups, conferring these nanocarriers with high molecular surface/volume ratios (Tomalia, 1991). G4 PAMAM-NH_2 dendrimers were shown earlier to bind electrostatically with different plasmid DNA vectors (Shakhbazau et al., 2012b; Shakhbazau et al., 2012c)and transfect a variety of target cells (Pandita et al., 2011; Santos et al., 2009; Shakhbazau *et al.*, 2012b; Shakhbazau et al., 2012d).

pLVHTM vector was chosen for this part of our study as it provides constitutive GFP expression under a strong EF1α promoter, making it a useful reporter plasmid. GFP has also been confirmed as a valid and stable morphological *in vivo* marker for Schwann cells seeded into bioengineered nerve conduit implants (Tohill et al., 2004). Moreover, pLVHTM is specifically designed for direct cloning of shRNAs, making it also a potential vehicle of interest in our efforts to develop dendrimer-based RNA interference approaches (Shcharbin et al., 2011; Weber et al., 2008). As the vectors of this family have not yet been validated for dendrimer complexation, we have first confirmed pLVHTM/PAMAM nanocomplex formation by established biophysical tests. Fluorescence intensity pattern in ethidium bromide displacement assay showed clear evidence of pLVHTM vector complexation upon addition of PAMAM dendrimers at different charge ratios, with zeta-potential of 5.93±0.46 mV at 5:1 ratio and zeta-size of the complexes depicted in Suppl. table 1.

In the subsequent proof-of-principle transfection experiments, we have demonstrated for the first time dendrimer transfection of primary SCs in two culture settings – traditional adherent culture, and 3D collagen-GAG matrix. A portion of dendriplex-exposed cells expressed plasmid-encoded GFP, while retaining their morphology and apparently (Fig. 5A) the capacity to divide. Gene delivery efficiencies were limited for both types of cell growth substrate but comparable with transfection rates for primary cells previously published by us and others (Santos *et al.*, 2009; Shakhbazau *et al.*, 2012b; Shakhbazau *et al.*, 2012c). As mentioned above, division rate was limited in matrix-embedded purified SCs, leading to further decrease in transfection rate (Fig. 5F). Nevertheless, our transfection experiments confirmed PAMAM ability to transfect SCs and the penetration of dendrimer complex into the 3D matrix structure, along with cell viability and a limited degree of permeability for transfection in a prospective cell substrate.

.

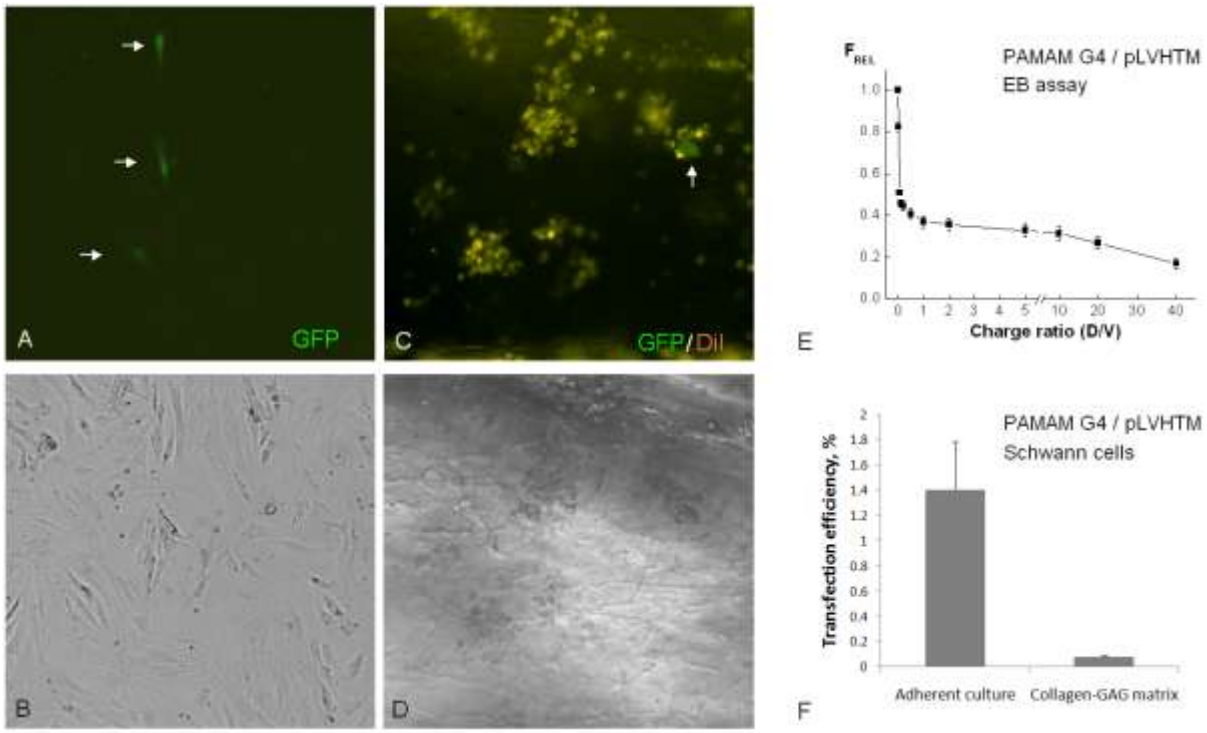

Figure 5. Schwann cells transfection by PAMAM dendrimers (100x magnification). A-B, SC transfection in adherent culture (A, fluorescence; B, transmitted light). C-D, transfection of DiI-labeled SC in the collagen-GAG matrix (A, fluorescence; B, transmitted light). Arrows indicate transfected cells. E, ethidium bromide displacement assay indicates vector/carrier binding: changes of fluorescence emission intensity of EB complexed with pLVHTM vector upon addition of PAMAM dendrimers at different charge ratios. $\lambda_{exc.}$ = 484 nm, $\lambda_{em.}$ = 601 nm. F, transfection rates in adherent culture and collagen-GAG matrix.

In summary, we have presented a model for *in vitro* and *in vivo* assessment of SC migration in the collagen-GAG matrix and confirmed its compatibility with dendrimer-driven SC transfection. Collagen-GAG matrix represents a prospective artificial substrate that confirms and closely mimics the recently established pattern of SC migration into the regenerating nerve in close cooperation with other cell types (Napoli *et al.*, 2012; Parrinello *et al.*, 2010). Our model also evaluates the prospect of matrix pre-seeding with cultured SC prior to implantation into the injured nerve. Taken together, these data offer a new aspect of the regenerative potential of this type of conduit.

Acknowledgements

This research was supported by CIHR grant #163322, by the Center for excellence in nerve regeneration (partnership between the Hotchkiss Brain Institute, University of Calgary and Integra LifeSciences), and by Alberta Innovates-Health Solutions (fellowship support for A.S.). The authors thank Ranjan Kumar and Indranil Dey for their kind assistance.

REFERENCES

1. Archibald, S.J., Krarup, C., Shefner, J., Li, S.T., Madison, R.D. (1991). A collagen-based nerve guide conduit for peripheral nerve repair: an electrophysiological study of nerve regeneration in rodents and nonhuman primates. J. Comp Neurol. 306**,** 685-696.

2. Archibald, S.J., Shefner, J., Krarup, C., Madison, R.D. (1995). Monkey median nerve repaired by nerve graft or collagen nerve guide tube. J. Neurosci. 15**,** 4109-4123.

3. Armstrong, S.J., Wiberg, M., Terenghi, G., Kingham, P.J. (2008). Laminin activates NF-kappaB in Schwann cells to enhance neurite outgrowth. Neurosci. Lett. 439**,** 42-46.

4. Bachelin, C., Zujovic, V., Buchet, D., Mallet, J., Baron-Van, E.A. (2010). Ectopic expression of polysialylated neural cell adhesion molecule in adult macaque Schwann cells promotes their migration and remyelination potential in the central nervous system. Brain 133**,** 406-420.

5. Belkas, J., Shoichet, M.S., Midha, R. Axonal Guidance Channels in Peripheral Nerve Regeneration. Operative techniques in Orthopaedics 14, 190-198. 2005.

Ref Type: Generic

6. Brushart, T.M.E., 1991. The mechanical and humoral control of specificity in nerve repair. In: Gelberman, R.H. (Ed.), Operative Nerve Repair and Reconstruction J.B. Lippincott, Philadelphia, pp. 215-230.

7. Chamberlain, L.J., Yannas, I.V., Hsu, H.P., Strichartz, G., Spector, M. (1998). Collagen-GAG substrate enhances the quality of nerve regeneration through collagen tubes up to level of autograft. Exp. Neurol. 154**,** 315-329.

8. Chamberlain, L.J., Yannas, I.V., Hsu, H.P., Strichartz, G.R., Spector, M. (2000). Near-terminus axonal structure and function following rat sciatic nerve regeneration through a collagen-GAG matrix in a ten-millimeter gap. J. Neurosci. Res. 60**,** 666-677.

9. Chen, Y.Y., McDonald, D., Cheng, C., Magnowski, B., Durand, J., Zochodne, D.W. (2005). Axon and Schwann cell partnership during nerve regrowth. J. Neuropathol. Exp. Neurol. 64**,** 613-622.

10. Fu, S.Y., Gordon, T. (1997). The cellular and molecular basis of peripheral nerve regeneration. Mol Neurobiol 14**,** 67-116.

11. Hanafi, A., Nograles, N., Abdullah, S., Shamsudin, M.N., Rosli, R. (2013). Cellulose acetate phthalate microencapsulation and delivery of plasmid DNA to the intestines. J. Pharm. Sci. 102**,** 617-626.

12. Harley, B.A., Kim, H.D., Zaman, M.H., Yannas, I.V., Lauffenburger, D.A., Gibson, L.J. (2008). Microarchitecture of three-dimensional scaffolds influences cell migration behavior via junction interactions. Biophys. J. 95**,** 4013-4024.

13. Harrisingh, M.C., Perez-Nadales, E., Parkinson, D.B., Malcolm, D.S., Mudge, A.W., Lloyd, A.C. (2004). The Ras/Raf/ERK signalling pathway drives Schwann cell dedifferentiation. EMBO J. 23**,** 3061-3071.

14. Hu, Y., Leaver, S.G., Plant, G.W., Hendriks, W.T., Niclou, S.P., Verhaagen, J., Harvey, A.R., Cui, Q. (2005). Lentiviral-mediated transfer of CNTF to schwann cells within reconstructed peripheral nerve grafts enhances adult retinal ganglion cell survival and axonal regeneration. Mol. Ther. 11**,** 906-915.

15. Hudson, A.R., Morris, J., Weddell, G., Drury, A. (1972). Peripheral nerve autografts. J Surg Res 12**,** 267-274.

16. Kemp, S.W.P., Syed, S., Walsh, S.K., Zochodne, D.W., Midha, R. (2009). Collagen Nerve Conduits Promote Enhanced Axonal Regeneration, Schwann Cell Association, and Neovascularization Compared to Silicone Conduits. Tissue Eng Part A.

17. Komiyama, T., Nakao, Y., Toyama, Y., Asou, H., Vacanti, C.A., Vacanti, M.P. (2003). A novel technique to isolate adult Schwann cells for an artificial nerve conduit. J. Neurosci. Methods 122**,** 195-200.

18. Lavdas, A.A., Franceschini, I., Dubois-Dalcq, M., Matsas, R. (2006). Schwann cells genetically engineered to express PSA show enhanced migratory potential without impairment of their myelinating ability in vitro. Glia 53**,** 868-878.

19. Lee, J.Y., Giusti, G., Friedrich, P.F., Archibald, S.J., Kemnitzer, J.E., Patel, J., Desai, N., Bishop, A.T., Shin, A.Y. (2012). The effect of collagen nerve conduits filled with collagen-glycosaminoglycan matrix on peripheral motor nerve regeneration in a rat model. J. Bone Joint Surg. Am. 94**,** 2084-2091.

20. Liu, J., Chau, C.H., Liu, H., Jang, B.R., Li, X., Chan, Y.S., Shum, D.K. (2006). Upregulation of chondroitin 6-sulphotransferase-1 facilitates Schwann cell migration during axonal growth. J. Cell Sci. 119**,** 933-942.

21. Luo, K., Li, C., Wang, G., Nie, Y., He, B., Wu, Y., Gu, Z. (2011). Peptide dendrimers as efficient and biocompatible gene delivery vectors: Synthesis and in vitro characterization. J. Control Release 155**,** 77-87.

22. Mandke, R., Singh, J. (2012). Effect of acyl chain length and unsaturation on physicochemical properties and transfection efficiency of N-acyl-substituted low-molecular-weight chitosan. J. Pharm. Sci. 101**,** 268-282.

23. Martini, R. (1994). Expression and functional roles of neural cell surface molecules and extracellular matrix components during development and regeneration of peripheral nerves. J. Neurocytol. 23**,** 1-28.

24. Millesi, H., Meissl, G., Berger, A. (1972). The interfasicular nerve-grafting of the median and ulnar nerves. J Bone Joint Surg Am 54-A**,** 727-750.

25. Napoli, I., Noon, L.A., Ribeiro, S., Kerai, A.P., Parrinello, S., Rosenberg, L.H., Collins, M.J., Harrisingh, M.C., White, I.J., Woodhoo, A., Lloyd, A.C. (2012). A central role for the ERK-signaling pathway in controlling Schwann cell plasticity and peripheral nerve regeneration in vivo. Neuron 73**,** 729-742.

26. Noble, J., Munro, C.A., Prasad, V.S.S.V., Midha, R. (1998). Analysis of upper and lower extremity peripheral nerve injuries in a population of patients with multiple injuries. J Trauma 45**,** 116-122.

27. Pandita, D., Santos, J.L., Rodrigues, J., Pego, A.P., Granja, P.L., Tomas, H. (2011). Gene delivery into mesenchymal stem cells: a biomimetic approach using RGD nanoclusters based on poly(amidoamine) dendrimers. Biomacromolecules. 12**,** 472-481.

28. Parrinello, S., Napoli, I., Ribeiro, S., Wingfield, D.P., Fedorova, M., Parkinson, D.B., Doddrell, R.D., Nakayama, M., Adams, R.H., Lloyd, A.C. (2010). EphB signaling directs peripheral nerve regeneration through Sox2-dependent Schwann cell sorting. Cell 143**,** 145-155.

29. Pieper, J.S., van Wachem, P.B., van Luyn, M.J.A., Brouwer, L.A., Hafmans, T., Veerkamp, J.H., van Kuppevelt, T.H. (2000). Attachment of glycosaminoglycans to collagenous matrices modulates the tissue response in rats. Biomaterials 21**,** 1689-1699.

30. Richardson, P.M. (1991). Neurotrophic factors in regeneration. Current Opinion in Neurobiology 1**,** 401-406.

31. Santos, J.L., Oramas, E., Pego, A.P., Granja, P.L., Tomas, H. (2009). Osteogenic differentiation of mesenchymal stem cells using PAMAM dendrimers as gene delivery vectors. J. Control Release 134**,** 141-148.

32. Schlosshauer, B., Dreesmann, L., Schaller, H.E., Sinis, N. (2007). Synthetic nerve guide implants in humans: a comprehensive survey. Neurosurgery 61**,** E1340.

33. Shakhbazau, A., Kawasoe, J., Hoyng, S.A., Kumar, R., Van, M.J., Verhaagen, J., Midha, R. (2012a). Early regenerative effects of NGF-transduced Schwann cells in peripheral nerve repair. Mol. Cell Neurosci. 50**,** 103-112.

34. Shakhbazau, A., Shcharbin, D., Bryszewska, M., Kumar, R., Wobma, H.M., Kallos, M.S., Goncharova, N., Seviaryn, I., Kosmacheva, S., Potapnev, M., Midha, R. (2012b). Non-viral engineering of skin precursor-derived Schwann cells for enhanced NT-3 production in adherent and microcarrier culture. Curr. Med. Chem. 19**,** 5572-5579.

35. Shakhbazau, A., Shcharbin, D., Petyovka, N., Goncharova, N., Seviaryn, I., Kosmacheva, S., Bryszewska, M., Potapnev, M. (2012c). Non-virally modified human mesenchymal stem cells produce ciliary neurotrophic factor in biodegradable fibrin-based 3D scaffolds. J. Pharm. Sci 101**,** 1546-1554.

36. Shakhbazau, A., Shcharbin, D., Seviaryn, I., Goncharova, N., Kosmacheva, S., Potapnev, M., Bryszewska, M., Kumar, R., Biernaskie, J., Midha, R. (2012d). Dendrimer-driven neurotrophin expression differs in temporal patterns between rodent and human stem cells. Mol. Pharm. 9**,** 1521-1528.

37. Sharma, G., Modgil, A., Sun, C., Singh, J. (2012). Grafting of cell-penetrating peptide to receptor-targeted liposomes improves their transfection efficiency and transport across blood-brain barrier model. J. Pharm. Sci. 101**,** 2468-2478.

38. Shcharbin, D., Pedziwiatr, E., Nowacka, O., Kumar, M., Zaborski, M., Ortega, P., de la Mata, F.J., Gomez, R., Munoz-Fernandez, M.A., Bryszewska, M. (2011). Carbosilane dendrimers NN8 and NN16 form a stable complex with siGAG1. Colloids Surf. B Biointerfaces. 83**,** 388-391.

39. Szulc, J., Wiznerowicz, M., Sauvain, M.O., Trono, D., Aebischer, P. (2006). A versatile tool for conditional gene expression and knockdown. Nat. Methods 3**,** 109-116.

40. Tohill, M.P., Mann, D.J., Mantovani, C.M., Wiberg, M., Terenghi, G. (2004). Green fluorescent protein is a stable morphological marker for schwann cell transplants in bioengineered nerve conduits. Tissue Eng 10**,** 1359-1367.

41. Tomalia, D.A. (1991). Dendrimer research. Science 252**,** 1231.

42. Walsh, S., Biernaskie, J., Kemp, S.W., Midha, R. (2009). Supplementation of acellular nerve grafts with skin derived precursor cells promotes peripheral nerve regeneration. Neuroscience 164**,** 1097-1107.

43. Webber, C., Zochodne, D. (2010). The nerve regenerative microenvironment: early behavior and partnership of axons and Schwann cells. Exp. Neurol. 223**,** 51-59.

44. Weber, N., Ortega, P., Clemente, M.I., Shcharbin, D., Bryszewska, M., de la Mata, F.J., Gomez, R., Munoz-Fernandez, M.A. (2008). Characterization of carbosilane dendrimers as effective carriers of siRNA to HIV-infected lymphocytes. J. Control Release 132**,** 55-64.

45. Weidner, N., Blesch, A., Grill, R.J., Tuszynski, M.H. (1999). Nerve growth factor-hypersecreting Schwann cell grafts augment and guide spinal cord axonal growth and remyelinate central nervous system axons in a phenotypically appropriate manner that correlates with expression of L1. J. Comp Neurol. 413**,** 495-506.

46. Yamada, Y., Hashida, M., Hayashi, Y., Tabata, M., Hyodo, M., Ara, M.N., Ohga, N., Hida, K., Harashima, H. (2013). An approach to transgene expression in liver endothelial cells using a liposome-based gene vector coated with hyaluronic acid. J. Pharm. Sci.

47. Yannas, I.V., Lee, E., Orgill, D.P., Skrabut, E.M., Murphy, G.F. (1989). Synthesis and characterization of a model extracellular matrix that induces partial regeneration of adult mammalian skin. Proc. Natl. Acad. Sci. U. S. A 86**,** 933-937.

48. Zhao, Q., Dahlin, L.B., Kanje, M., Lundborg, G. (1992). The formation of a 'pseudo-nerve' in silicone chambers in the absence of regenerating axons. Brain Res. 592**,** 106-114.

49. Zochodne, D. Neurobiology of Peripheral Nerve Regeneration, First Edition (New York: Cambridge University Press). 2008.

Ref Type: Generic